



Structural and Optical Properties of a Gallium-doped Zinc Oxide Thin Film Deposited by Dip Coating

Modou Pilor^{2,1}, Bouchaib Hartiti¹, Papa Touty Traore², Alassane Diaw², Awa Dieye², Moulaye Diagne², Bassirou Ba², Phillipe thevenin³

¹ERDyS Laboratory, GMEEM & DD Group, Hassan II University of Casablanca, FSTM, Morocco

²LASES laboratory, Cheikh Anta Diop University of Dakar, Sénégal

³University of Lorraine, LMOPS, Metz, France

Abstract In this work we studied the optical and structural properties of a gallium-doped zinc oxide layer deposited by the sol gel method in combination with dip coating. The optimal deposition conditions were obtained from previous studies using Taguchi's design of experiments. For the characterisation we used X-ray diffraction (XRD). This characterisation allowed us to study the effect of the gallium doping rate on the structural properties of the ZnO layer. We also used UV-Visible spectrophotometry to plot the transmittance of the layer. All transmittance spectra showed clear absorption profiles in the wavelength range between 360 and 400 nm. GZO thin films with Ga doping levels above 2% showed average transmittance values higher than 91%, and Ga-doped thin films with 3% doping showed the best average transmittance, 92.1%. The value of E_g for undoped ZnO thin films was 3,23 eV, which is consistent with our previous report 18 and the value of E_g for Ga-doped samples was 3,25 eV, slightly higher than that of undoped samples. The blue shift of optical bandgap for the doped ZnO thin films is due to the increase in carrier concentration, which leads to a broadening of the energy band.

Keywords Zinc oxide (ZnO), structural properties, optical properties, gallium doping concentration

Introduction

Zinc Oxide (ZnO) is a material commonly used in electronic circuits due to its wide direct band gap of 3.37 eV, high exciton binding energy of approximately 60 meV, non-toxic nature, high electron mobility, and excellent piezoelectric behavior [1]. ZnO has various applications such as gas sensors [2], photodiodes [3], solar cells [4], optical modulator waveguides [5], photonic crystals [6], varistors [7], and more. Different methods can be used to produce ZnO thin films, including chemical bath deposition [8], sol-gel combined with spin coating [9], sol-gel dip coating [10], spray pyrolysis [11], sputtering magnetron [12], electrodeposition [13], etc. Out of these techniques, sol-gel dip-coating is a popular method as it is easy to perform, and allows the production of high-quality films with good properties at a low cost [14]. The main goal of this technique is to achieve a uniform thin film thickness and distribution at high yield and low production cost [15]

The main aim of this work is to study the concentration gallium doping effect on the optimal zinc oxide layer. The ZnO films deposited at the optimized conditions are obtained by Taguchi method [16]. The optical and structural properties of this optimal layer doped with various concentrations of gallium is investigated in this work



Experimental Part

In this section, we study the effect of gallium doping on the properties of zinc oxide. To do this, we prepared a ZnO layer using the optimal conditions obtained previously with the Taguchi method. The nanohydrated gallium nitrate $[\text{Ga}(\text{NO}_3)_3 \cdot 9\text{H}_2\text{O}]$ was chosen as the source of gallium dopant. Gallium concentrations were varied from 0 to 5% (in steps of 1%) and were slowly added to the $[\text{Ga}(\text{NO}_3)_3 \cdot 9\text{H}_2\text{O}]$ solution before being homogeneously mixed by a magnetic stirrer for 90 minutes at 60°C . The sol-gel deposition method was used in combination with dip coating.

X-ray diffraction (XRD) and UV-visible characterization allowed us to do the following investigations

Results & Discussion

Transmittance of gallium-doped thin films

The optical transmittance spectra of undoped and gallium-doped thin films in the ultraviolet and visible domains are presented in the figure. All transmittance spectra showed clear absorption profiles in the wavelength range between 360 and 400 nm, and these absorption profiles shifted towards shorter wavelengths (blue shift) when gallium was incorporated into the ZnO films. Similar behavior was also observed by Rao et al. for transparent conductive Gallium doped Zinc Oxide thin films prepared by spray pyrolysis technique [16]. The magnitudes of the shifts increased proportionally with the amount of Ga. Furthermore, all Ga-doped samples exhibited higher transparency than the undoped ZnO sample (Figure 1). The average transmittance values of Gallium doped Zinc Oxide thin films were calculated for wavelengths between 500 and 800 nm. Gallium doped Zinc Oxide thin films with Ga doping levels above 2% showed average transmittance values higher than 91%, and Ga-doped thin films with 3% doping showed the best average transmittance, 92.1%. Lee et al. reported that the optical properties of sol-gel-derived ZnO films were mainly affected by the surface morphology [17]. The transmittance of ZnO thin films in the visible light region was also affected by the film thickness, grain size, and defects (such as nanopores and nanovoids). The transmittance of 5% Ga-doped films was lower than that of 3% Ga-doped films. This result may be due to the degradation of film quality and the increase in the number of nanopores in the films caused by the high level of Ga doping.

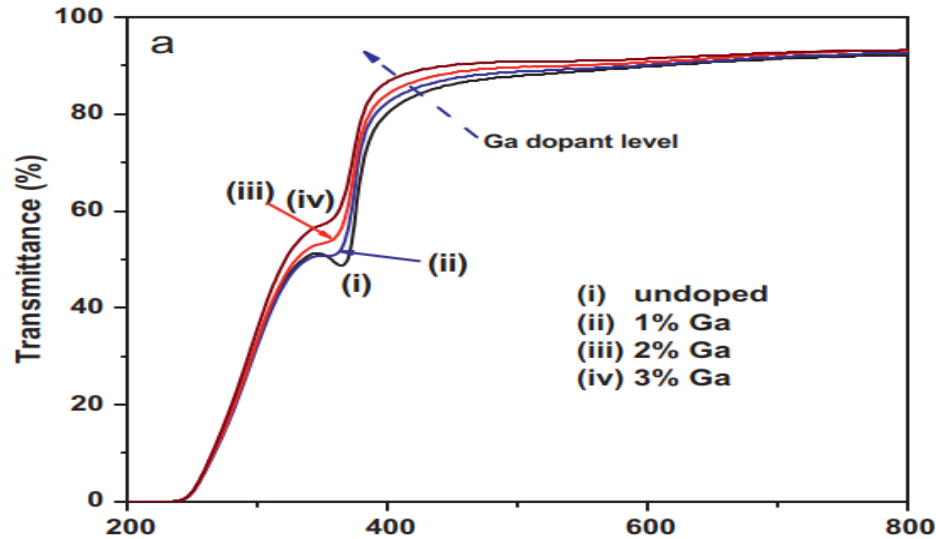


Fig. 1 Transmittance spectra of gallium doped ZnO

Bandgap energy

In this section, we study the effect of gallium doping on the bandgap energy of zinc oxide thin films. For this purpose, we prepared ZnO films under optimal conditions obtained previously in our work using Taguchi method [16]

$$\alpha = \frac{1}{t} \ln \left(\frac{I_0}{I} \right) \quad (\text{Eq. 1})$$



where t is the thickness of the film and the T the transmittance. The value of E_g for undoped ZnO thin films was 3.23 eV, which is consistent with our previous report [18] and the value of E_g for Ga-doped samples was 3.25 eV, slightly higher than that of undoped samples. The blue shift of optical bandgap for the doped ZnO thin films is due to the increase in carrier concentration, which leads to a broadening of the energy band [19,20]. Kalaivanan et al. showed that the broadening of the optical bandgap could be attributed mainly to the increase in disorder of the polycrystalline semiconductor films, which leads to the appearance of localized electron and the hole states [21]. Such a transparent semiconductor oxide (TCO) thin film could be applied as an active channel layer in transparent thin film transistor

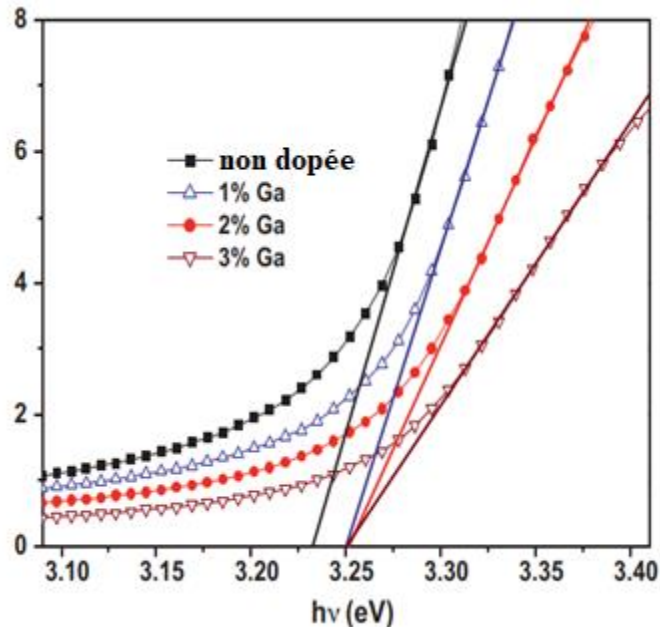


Figure 2: bandgap energy function of gallium doping rate

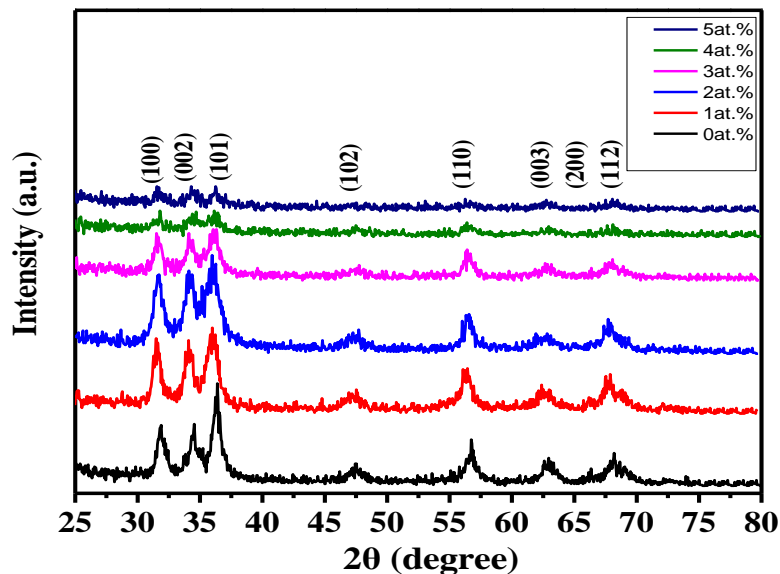


Figure 3: XRD chraterization of gallium doped zinc oxide samples

The XRD results showed that all prepared ZnO films were polycrystalline with a hexagonal wurtzite structure. The diffraction peaks tend to decrease with increasing Ga dopant concentrations. The diffraction signals of the (102) and (103) planes are very weak for high concentrations of Ga doping. At higher levels of Ga doping, the crystalline qualities of the ZnO thin films are degraded. Nishino et al. showed that this degradation can be



caused by the influence of constraints resulting from the difference between the ionic radii of zinc and dopant ions [22]. In addition, the XRD patterns indicated that the 5% Ga-doped ZnO thin films had a rather amorphous nature. The preferred growth orientation of polycrystalline thin films can be understood from the texture coefficient $TC(hkl)$ for all planes. The texture coefficient of the $(h\ k\ l)$ plane is calculated using the following equation [23,24].

$$TC_{(hkl)} = \frac{I_{(hkl)}}{Ir_{(hkl)}} \left[\frac{1}{n} \sum \frac{I_{(hkl)}}{Ir_{(hkl)}} \right] \quad (\text{Eq. 2})$$

where $I(hkl)$ is the DRX intensity obtained from the films, n is the number of diffraction peaks considered, and $Ir(hkl)$ is the intensity of the reference XRD patterns (JCP).

The reference XRD patterns (JCPDS 36-1451 card). Table 1 shows the variation of the texture coefficient of the series of thin GZO films with Ga dopant concentration. The relatively higher values of texture coefficient are along the (002) plane for all films. $I(hkl)$ is the DRX intensity obtained from the films, n is the number of diffraction peaks considered, and $Ir(hkl)$ is the intensity of the reference XRD patterns (JCP).

The reference XRD patterns (JCPDS 36-1451 card). Table 1 shows the variation of the texture coefficient of the series of thin GZO films with Ga dopant concentration. The relatively higher values of texture coefficient are along the (002) plane for all films.

Table 1: Variation du coefficient de texture en fonction du pourcentage de dopage

Concentration of Ga doping (%)	Texture coefficient (TC (hkl))				
	(100)	(002)	(101)	(102)	(110)
0	1,10	1,53	0,90	0,65	1,06
1	1,18	1,60	0,82	0,79	0,76
2	1,22	1,33	0,93	0,91	0,93
3	0,85	1,22	0,94	1,03	0,96

This indicates that the Gallium doped Zinc Oxide thin films had a preferential orientation along the (002) plane. Doping the thin ZnO films with gallium increased the full-width at half-maximum (FWHM) of the (100), (002) and (101) peaks, indicating that Ga doping reduced the crystallite size of the thin Gallium doped Zinc Oxide films. The crystallite sizes of the films were estimated by the Scherrer formula. The average crystallite sizes of undoped ZnO and 1% Ga-doped ZnO were estimated by the Scherrer formula.

The interplanar distance d_{hkl} is calculated from the Bragg formula (Eq.3)

$$2d_{hkl} \sin \theta = n\lambda \quad (\text{Eq. 3})$$

θ diffraction angle

n diffraction order

λ wavelength

we calculated some parameters in the table 2 like the crystallite size (D_{hkl}), the lattice parameters a et c for different gallium doping concentration.

$$D_{hkl} = 0,9 \frac{\lambda}{\beta \cos \theta} \quad (\text{Eq. 4})$$

$$\frac{1}{d_{hkl}^2} = \frac{4}{3} \left(\frac{h^2 + hk + k^2}{a^2} \right) + \frac{l^2}{c^2} \quad (\text{Eq. 5})$$



Table 2: Parameters and crystallite size

Level of Ga doping (%)	FWHM (101) $\times 10^{-3}$ (rad)	crystallite size (nm)	<i>a</i> (Å)	<i>c</i> (Å)	<i>c/a</i>
0.00	2.7022	56.39	3.2496	5.2066	1.60222
1.00	3.0641	49.73	3.2498	5.2067	1.60216
2.00	3.4443	44.24	3.2499	5.2069	1.60217
3.00	3.6305	41.97	3.2501	5.2070	1.60210

The thin films of 1% Ga-doped ZnO for the three main diffraction peaks in the (100), (002) and (101) planes were 24.3 and 20.8 nm, respectively. When the Ga dopant concentrations were increased from 2 to 5%, the average crystallite size decreased from 18.2 to 12.2 nm.

Conclusion

The prepared samples were analysed by two types of techniques: X-ray diffraction technique and UV-visible. The structural study made by X-ray diffraction of our samples showed that all the ZnO films obtained are polycrystalline with a hexagonal wurtzite structure of high intensity in the [002] preferential direction perpendicular to the surface of the glass substrates. The optical transmittance is above 90% in the visible region and the graphically determined optical gap is 3.287 eV.

All X-ray diffraction spectra of our samples showed polycrystalline growth where all peaks observed correspond to the hexagonal wurtzite structure of ZnO with a preferential orientation along the [002] direction. UV-visible optical characterisation by spectrophotometry showed that all thin films have a high optical transmission of about 90% in the visible range. A decrease in the energy E_g was observed when increasing the dopant concentration, which may be due to electronic impurities in the ZnO matrix.

References

- [1]. K. D. Kim, D. W. Choi, Y. H. Choa, H. T. Kim "Optimization of parameters for the synthesis of zinc oxide nanoparticles by Taguchi robust design method" Colloids and surfaces A, vol. 311, pp. 170-173, June 2007
- [2]. P. Mitra, A.P. Chatterjee, H.S. Maiti (1997) ZnO thin film gas sensor, Materials Letters 35 (1998) 33-38
- [3]. J.Y. Lee, Y.S. Choi, J.H. Kim, M.O. Park, S. Im Optimizing n-ZnO/p-Si heterojunction for photodiode applications Thin solid Films 403-404 (2002) 553-557
- [4]. Michael Gratzal, Dye-Sensitized Solid-state heterojunction solar cell www.mrs.org/pbmications/bulletin volume 30 2005
- [5]. M H Koch, P Y Timbrell and R N Lamb the influence of thin film cristallinty on coupling efficiency of ZnO optical modulator waveguides 1995
- [6]. Yefan Chen, Darren Bagnall, Takafumi Yao ZnO as a novel photonic material for UV region Materials Science and Engineering B75 (2000) 190-198
- [7]. Yuanhuan Lin, Zhongtai Zhang, Zilong Tang, Fangli Yuan and Jinlin Li Characterisation of ZnO-based Varistore prepared from nanometer precursor powders Advanced Materials for Optics and Electronics Adv. Mater. Opt. Electron. 9, 205-209 (1999)
- [8]. Y.F Wang, J.H Yao, D.Jia and H. Lei Optical prosperities of Ag-ZnO Composition nanofilms synthesized by Chemical bath deposition Acta Physica Polonia A (2010)
- [9]. Jin-Hong Lee, Kyung-Hee Ko, Byung-Ok Park Electrical and optical properties of ZnO transparent conducting films by sol-gel method Journal of Crystal Growth 247 (2003) 119-125
- [10]. Zohra N. Kayani, Fareeha Naz, Saira Riaz, Shahzad Nasseem Characteristics of Al doped ZnO: Ni grown on glass substrate by sol-gel dip coating technique Journal of Saudi Chemical Society Volume 21, issue 4, May 2017 Pages 425-433



- [11]. F. Z. Bedia, A. Bedia, B. Benyoucef and S. Hamzaoui Electrical characterization of n-ZnO/p-Si heterojunction prepared by spray pyrolysis technique *Physics Procedia* 55(2014) 61-67 Eighth International Conference on Materials Sciences, CSM8-IS5 Ismail, M.J.
- [12]. Abdullah The structural and optical properties of ZnO thin films prepared at different RF sputtering power *Journal of King Saud University-Science* 2012
- [13]. J.H. Lee, K.H. Ko, B.O. Park, *J. Cryst. Growth* 247 (2003) 119–125.
- [14]. M. Nirmala, A. Anukaliani Structural and optical properties of an undoped and Mn doped ZnO nanocrystalline thin film *Photonics Letters of Poland* Vol. 2 (4) 189-191 (2010)
- [15]. E. Musavi, M. Khanlary, Z. Khakpour. Red-orange photoluminescence emission of sol-gel dip-coated prepared ZnO and ZnO:Al nano-crystalline films *Journal of Luminescence* 216 (2019)
- [16]. Modou Pilor, Bouchaib Hartiti, Alle Dioum, Hicham Labrim, Youssef Arba, Amine Belafhaili, Mounia Tahri, Salah Fadili, Bassirou Ba, Philippe Thevenin, The Use of Taguchi Method to Elaborate Good ZnO Thin Films by Sol Gel Associated to Dip Coating, *International Journal of Materials Science and Applications* 2021; 10(1): 18-24.
- [17]. T.P. Rao, M.C.S. Kumar, *J. Alloys Compd.* 506 (2010) 788–793.
- [18]. J.H. Lee, K.H. Ko, B.O. Park, *J. Cryst. Growth* 247 (2003) 119–125.
- [19]. C.Y. Tsay, H.C. Cheng, Y.T. Tung, W.H. Tuan, C.K. Lin, *Thin Solid Films* 517 (2008)
- [20]. Tahmineh Movahedi, Reza Norouzebeigi Synthesis of flower-like micro nano ZnO superhydrophobic surfaces: Additive effect optimization via designed experiments. *Journal of Alloys and Compounds* 795 (2019) 483-492.
- [21]. Xiujuan Chen, Gordon Huang, Chunjiang An, Renfei Feng, Yinghui Wu, Charley Huang Plasma-induced PAA-ZnO coated PVDF membrane for oily wastewater treatment: preparation, optimization and characterization through Taguchi OA design and synchrotron-based X-ray analysis *Journal of Membrane Science* (2019).
- [22]. A. Kalaivanan, S. Perumal, N.N. Pillai, K.R. Murali, *Mater. Sci. Semicond. Process.* 14 (2011) 94–96.
- [23]. K. F. Konan, B. Hartiti, B. Aka, A. Ridah, K. Dakhsi, Y. Arba et P. Thevenin Propriétés structurales et optiques de couches minces d'oxyde de zinc (ZnO) textures (002) par voie sol-gel via spin coating *Afrique Sciences* 06(1)(2010)29-37.
- [24]. J. Nishino, S. Ohshio, K. Kamata, *J. Am. Ceram. Soc.* 75 (1992) 3469–3472.
- [25]. T.P. Rao, M.C.S. Kumar, *J. Alloys Compd.* 506 (2010) 788–793.

